Ohmic contacts to n-type GaAs

W. J. Boudville and T. C. McGill
California Institute of Technology, Pasadena, California 91125

(Received 24 April 1985; accepted 25 April 1985)

We present a model of the metal–semiconductor junction, for heavily doped GaAs, so that tunneling dominates the current. It is assumed that the imaginary part of the wave vector in the semiconductor is given by the two-band model. Modifications in the barrier potential due to image charge, negative charge near the interface, and the degenerate doping of the semiconductor are included. The role of the L-point minimum in the GaAs in determining the position of the Fermi level in the semiconductor is included. The energy distribution of the conductance as a function of doping and barrier height is given. The contact resistance as a function of doping and barrier height is also presented. The results suggest that previous calculations are substantially in error due to the simple models that were used for the dependence of the imaginary part of the wave vector on energy.

I. INTRODUCTION

The development of GaAs technology has led to a continuing search for methods of making Ohmic contacts to n-type GaAs. One of the very interesting recent developments has been the growth of heavily doped layers using molecular beam epitaxy (MBE).[1] Furthermore, the most widely used theory of Ohmic contacts is that due to Chang, Fang, and Sze (CFS),[2] in which a metal–semiconductor contact is treated. Attempts to compare theory with experiment have been mainly based on this theory.[3,4,5]

In CFS's theory, they treat the tunneling of carriers through a Schottky barrier as a function of doping in the semiconductor. The theory includes the correction of the image potential to the barrier. It assumes that the tunneling through the barrier is characterized by an imaginary wave vector vs energy that is simple parabolic (one-band) relationship. Given the current interest in the theory, it is desirable to improve the theory so that it treats the best model available. With these improved results, one might hope for a more realistic comparison between the theory and experiment.

In this paper, we present the results of a more realistic treatment of the contact resistance for electrons tunneling through the Schottky barrier between a metal and GaAs, which is heavily doped n type. The theory includes the effects of image charge, negative charge at the interface, and the presence of the L-point minimum in the GaAs. The biggest correction is due to the improvement in the model of the imaginary wave vector vs energy relation. We assume a two-band model that uses the correct energy gap and conduction band effective mass for GaAs. We find results for the contact resistance which differ by as much as an order of magnitude in the doping ranges of interest for devices.

This paper is organized in the following way. Section II presents the theoretical model. In Sec. III we give the results for the model, and compare them with CFS. In Sec. IV, we show an example of fluctuations in the barrier potential due to the discrete nature of the doping. Finally, in Sec. V we present our conclusions.

II. THEORY

For a metal-n-semiconductor junction in reverse bias, with the semiconductor being degenerate, the energy diagram is shown in Fig. 1.

The corrections due to the image force,[6] negative charge at the interface,[7] and nonparabolic corrections to the potential due to the presence of conduction electrons[8] in part of the depletion region are all included. The metal is modeled as a degenerate electron gas, with the radius of the Fermi sphere (the Fermi energy) being ~7–8 eV. (This is not shown in Fig. 1, as it would be offscale.)

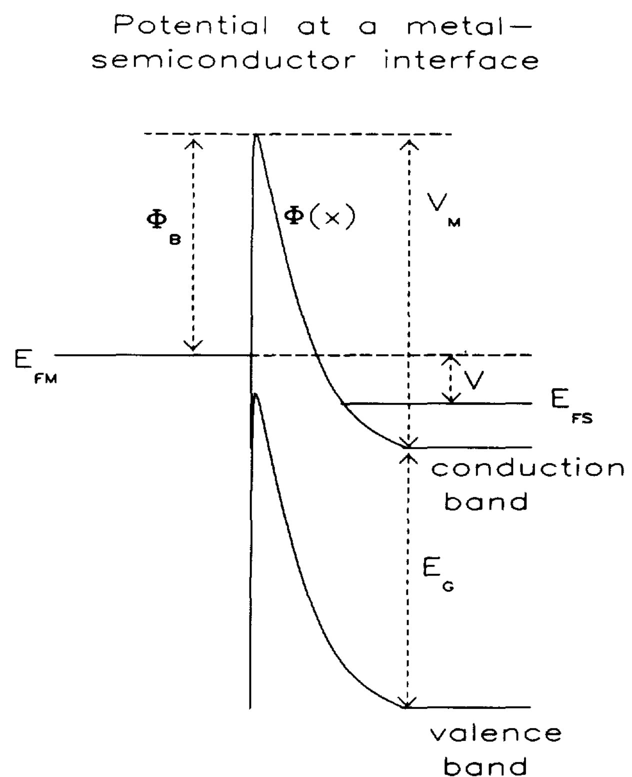

FIG. 1. Diagram of a metal-n-semiconductor junction for an applied bias V.

 0734-211X/85/041192-05$01.00 © 1985 American Vacuum Society

In Fig. 1, the energy is measured upwards from the conduction band edge far from the depletion region; E_{FS}, E_{FM} are the Fermi levels in the semiconductor and metal, respectively, and V is the applied bias. Then, following Ref. 9,

$$J=\frac{m_C k_B T q}{2\pi^2\hbar^3}\int_0^\infty dE\,T(E)\times\ln\left(\frac{\exp[-(E-E_{FS})/k_BT]+1}{\exp[-(E-E_{FM})/k_BT]+1}\right), \quad (1)$$

where E is the energy of electron normal to interface, m_C is the conduction band effective mass at the Γ point, and $T(E)$ is the transmission probability. Equation (1) neglects phonon-assisted processes, i.e., the transverse wave vector k is assumed to be conserved for tunneling particle. The large Fermi radius of the metal in reciprocal space, relative to the distribution of free carriers in reciprocal space for doped GaAs, or indeed most semiconductors, makes this a good approximation.[10] In the derivation of Eq. (1), a number of other approximations have been made. These approximations are detailed in Ref. 11. The approximations are very commonly made in treating a Schottky barrier and are not likely to result in large errors. One major assumption is used to guarantee that zero current will result when zero voltage is applied, by assuming that the boundary conditions on the current from the semiconductor to the metal are appropriate for the current in the other direction.

By the WKB approximation, take

$$T(E)=\begin{cases}\exp\left(-2i\int_{x_1}^{x_2}k(x)dx\right), & \text{if } 0<E<qV_m,\\ 1, & E>qV_m.\end{cases} \quad (2)$$

where x_1 and x_2 are the turning points of the forbidden region for k. Assuming a direct-gap semiconductor, a two-band model, from $k\cdot p$ theory, gives for k everywhere within the forbidden region,[12]

$$k=-i\left\{\frac{2m_C}{\hbar^2E_g}[\phi(x)-E][E_g+E-\phi(x)]\right\}^{1/2}, \quad (3)$$

$$\frac{1}{R_c}\equiv\frac{\partial J}{\partial V}\equiv\int_0^\infty dE\,G(E). \quad (4)$$

R_c is the specific contact resistance of the interface, measured in Ω cm^2, and $G(E)$ is the conductance distribution function. (Often, in the literature, R_c is defined at $V=0$, but there is no need to confine ourselves to this.) Then,

$$\frac{1}{R_c}=\frac{m_Cq^2}{2\pi^2\hbar^3}\int_0^\infty dE\frac{T(E)}{\exp[(E-E_{FM})/k_BT]+1}+\frac{m_C^2q^2k_BT}{\pi^2\hbar^5E_g}\times\int_0^{qV_m}dE\,T(E)\ln\left(\frac{\exp[-(E-E_{FM})/k_BT]+1}{\exp[-(E-E_{FS})/k_BT]+1}\right)\times\int_{x_1}^{x_2}dx\frac{[-E_g-2E+2\phi(x)]}{k(x)}. \quad (5)$$

R_c and $G(E)$ are found from Eq. (5) by numerical methods. [Note that at zero bias the second term in Eq. (5) is 0.] To obtain E_{FS} in Eq. (5), n, the free carrier concentration, is compared with N_C, the effective density of states in the conduction band. We assume that T is sufficiently large to neglect carrier freezeout. Then

$$E_{FS}=\begin{cases}k_BT\ln(n/N_C), & n<N_C,\\ \frac{\hbar^2}{2m_C}(3\pi^2n)^{2/3}, & n>N_C.\end{cases} \quad (6)$$

For carrier concentrations in the GaAs sufficiently large such that the L-point states are occupied, the semiconductor Fermi level is given by

$$n=\frac{1}{3\pi^2}\left[\left(\frac{2m_C}{\hbar^2}\right)^{3/2}E_{FS}^{3/2}+4\left(\frac{2m_L}{\hbar^2}\right)^{3/2}(E_{FS}-E_{\Gamma L})^{3/2}\right], \quad (7)$$

where m_L is the effective mass at the L point, and $E_{\Gamma L}$ is the energy separation between the L point and the Γ point. The factor of 4 in the second term on right-hand side of Eq. (7) arises because each Brillouin zone has a net of four L points.

The potential energy of the electron is given by

$$\phi(x)=-\frac{q^2}{16\pi\epsilon x}+\phi_1(x), \quad (8)$$

where, for degenerate doping, ϕ_1 satisfies the implicit relationships

$$\frac{d^2\phi_1}{dx^2}=\frac{q^2}{\epsilon}[n-n_e(x)] \quad (9)$$

$$n_e(x)=\begin{cases}\frac{1}{3\pi^2}\left\{\left[\left(\frac{2m_C}{\hbar^2}\right)(E_{FS}-\phi_1)\right]^{3/2}+4\left[\left(\frac{2m_L}{\hbar^2}\right)(E_{FS}-\phi_1-E_{\Gamma L})\right]^{3/2}\right\}, & E_{FS}-\phi_1>E_{\Gamma L},\\ \frac{1}{3\pi^2}\left[\left(\frac{2m_C}{\hbar^2}\right)(E_{FS}-\phi_1)\right]^{3/2}, & E_{FS}-\phi_1<E_{\Gamma L}.\end{cases} \quad (10)$$

For nondegenerate doping, where $E_{FS}<0$, let $n_e\equiv0$. Equations (9) and (10) are solved for ϕ_1 by the method of successive integration.[13] In doing this, the boundary condition of $\phi_1(x)=0$ at $x=1.2\times$ the depletion length is chosen to ensure convergence. The complete solution for ϕ_1 would tend to 0 asymptotically as $x\rightarrow\infty$. Thus the boundary condition lowers ϕ_1 near the edge of the depletion region. However, this occurs at large tunneling distances, relative to the tunneling distances at higher energies, and so will have little effect on the results.

The effect of negatively charged surface states can be included by adding the following term to the right-hand side of Eq. (8):

$$\phi_{surf}(x)=-\frac{dq^2N}{\epsilon}\exp(-x/d), \quad (11)$$

where N is the area density of surface states and d is the penetration length of the states.

III. RESULTS AND DISCUSSION

We have used the following values for the parameters in the theory: $T=300$ K, $E_G=1.42$ eV, $E_{\Gamma L}=0.284$ eV,

$m_C = 0.063$, $m_L = 0.55$, $\epsilon = 12.85$, and $N_C = 4.21 \times 10^{17}$ cm^{-3}. The value of E_G is taken from Ref. 14, while the other values are taken from Ref. 15.

To illustrate the contributions to the conductance per unit area per unit energy, for various doping concentrations, we have plotted in Fig. 2 the barrier shapes and values of $G(E)$ for four different dopings: 10^{17}, 10^{18}, 10^{19}, and 10^{20} cm^{-3}. These are at $\phi_{BO} = 0.8$ eV, $T = 300$ K, and $V = 0$ V. Negative surface charges are included, with the choice of $N = 5\times10^{14}$ cm^{-2}, $d = 5$ Å. $G(E)$ is plotted on a log scale due to its large variation when the energy is varied from 0 to 1 eV. For example, at a doping of 10^{19} cm^{-3}, $G(E)$ ranges over 10 orders of magnitude. Notice that $G(E)$ has a discontinuity in its slope at $E = qV_m$. This is due to Eq. (2), where the transmission below the barrier is given by the WKB approximation, while the transmission above the barrier was taken to be 1.

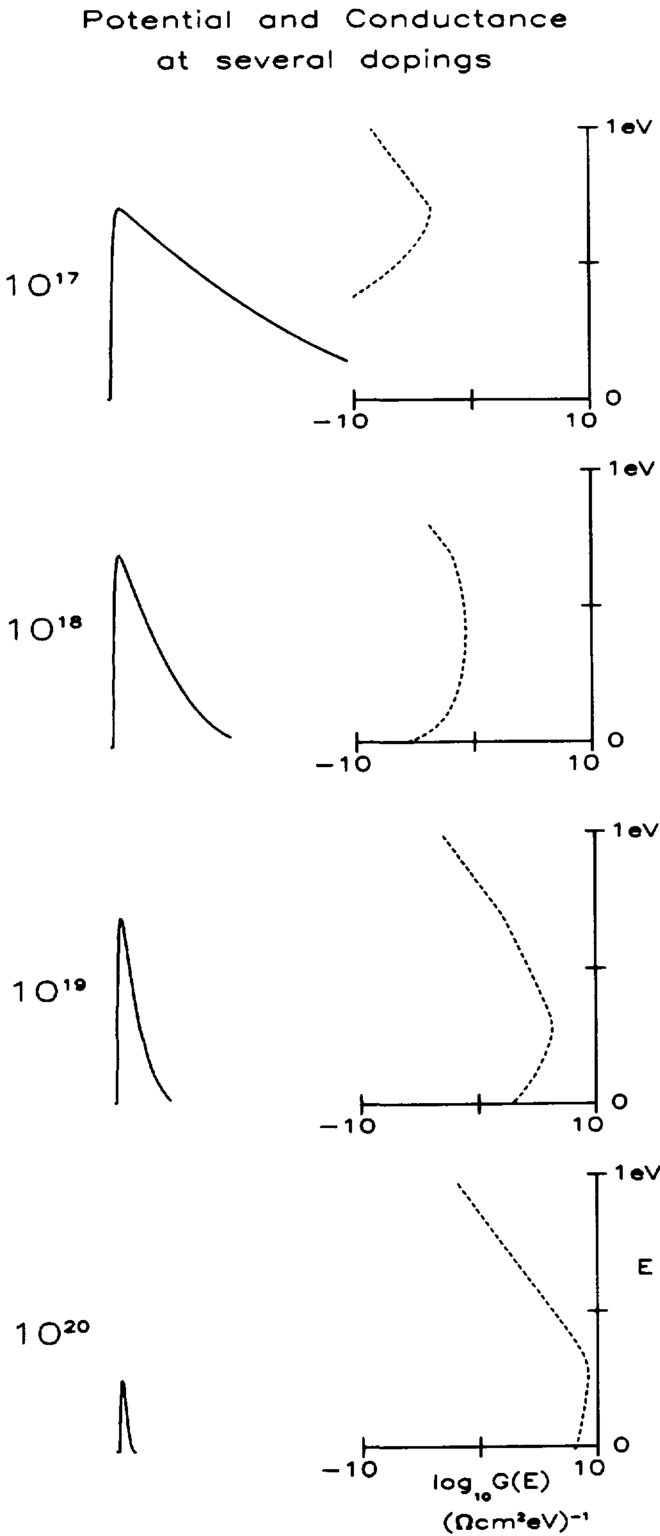

FIG. 2. Distributions of the specific contact conductance as a function of energy. To illustrate the energy position on the barrier, the barrier shape is plotted using the same energy scale. The log of the conductance is shown, with the conductance being measured in Ω^{-1} m^{-2} J^{-1}.

For a doping of 10^{17} cm^{-3}, the maximum in $G(E)$ occurs at qV_m, and the total conductance has roughly equal contributions from carriers going over the barrier in thermionic emission and Fowler–Nordheim tunneling.[16] Observe that the tunneling contribution is significant only for energies down to ~0.2 eV below qV_m, since the tunneling length increases strongly for decreasing energy. There is no direct tunneling, since $E_{FM} = E_{FS} < 0$. At a doping of 10^{18} cm^{-3} the maximum in $G(E)$ increases and it occurs at $E = 0.42$ eV, which is below qV_m. Due to the narrowing of the barrier, we get significant conductance over most of the tunneling energies. Fowler–Nordheim tunneling dominates the conductance, while some direct tunneling occurs, for $E < E_{FS} = 0.06$ eV. When the doping is raised to 10^{19} cm^{-3}, $G(E)$ increases strongly, with its maximum occurring at $E = 0.27$ eV$\simeq E_{FS}$. Now direct tunneling is comparable to Fowler–Nordheim tunneling. Finally, for a doping of 10^{20} cm^{-3}, V_m falls con-

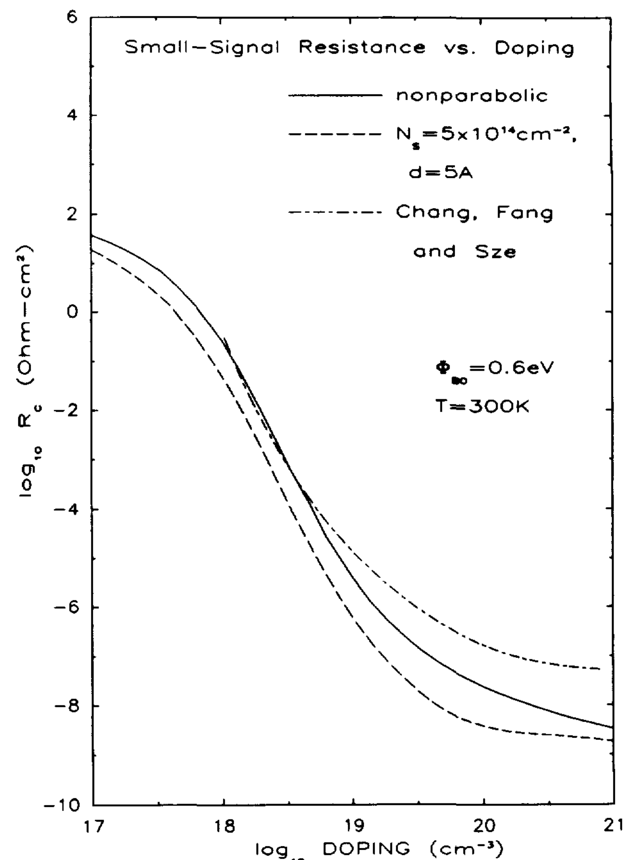

FIG. 3. Specific contact resistance vs doping, for $\phi_B = 0.6$ eV and $V = 0$ V, with and without negative surface charge, with the results from CFS.

siderably after being approximately constant at lower dopings. This is due to the negative surface states "annulling" most of the thin barrier. Here $E_{FS} = 0.33$ eV, and so, direct tunneling is seen to dominate the conductance.

The specific contact resistance as a function of doping is presented for three different intrinsic barrier heights: 0.6, 0.8, and 1.0 eV in Figs. 3–5, respectively. Our results include all of the effects described above. For comparison we have plotted the results assuming no negative surface charge, and also those from CFS. In Fig. 4, where $\phi_{B0} = 0.8$ eV, we also show the parabolic result. This occurs if in Eq. (10) we set $n_e \equiv 0$, regardless of whether or not the semiconductor is degenerately doped.

Comparison of the results in these figures allows us to draw a number of conclusions. First, let us describe those which are common to both CFS's and our models. The contact resistance is seen to increase as the barrier height increases, at fixed doping. For example, at a doping of 10^{19} cm^{-3}, in going from $\phi_{B0} = 0.6$ to 1.0 eV, the contact resistance increases by about two orders of magnitude in both models. For dopings between 10^{18} and 10^{19} cm^{-3}, the contact resistance falls steeply by about seven orders of magnitude. Recall from Fig. 2 and the discussion above, that over this doping range for $\phi_{B0} = 0.8$ eV, tunneling increased to dominate the total conductance, and $G(E)$ increased strongly over all the tunneling energies. Similar results are seen in our

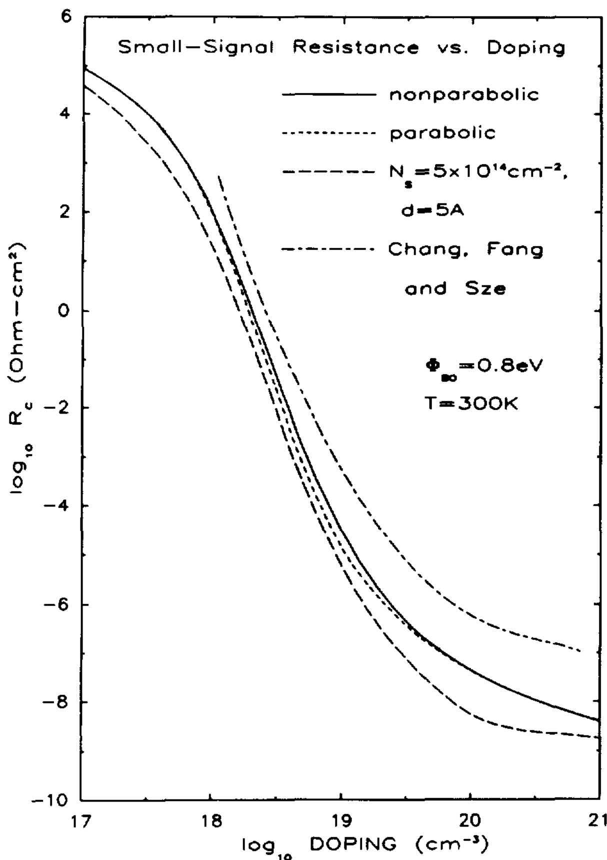

FIG. 4. Specific contact resistance vs doping, for $\phi_B = 0.8$ eV and $V = 0$ V, with and without negative surface charge, with the results from CFS. For comparison, the results assuming a parabolic conduction band in the depletion region are shown.

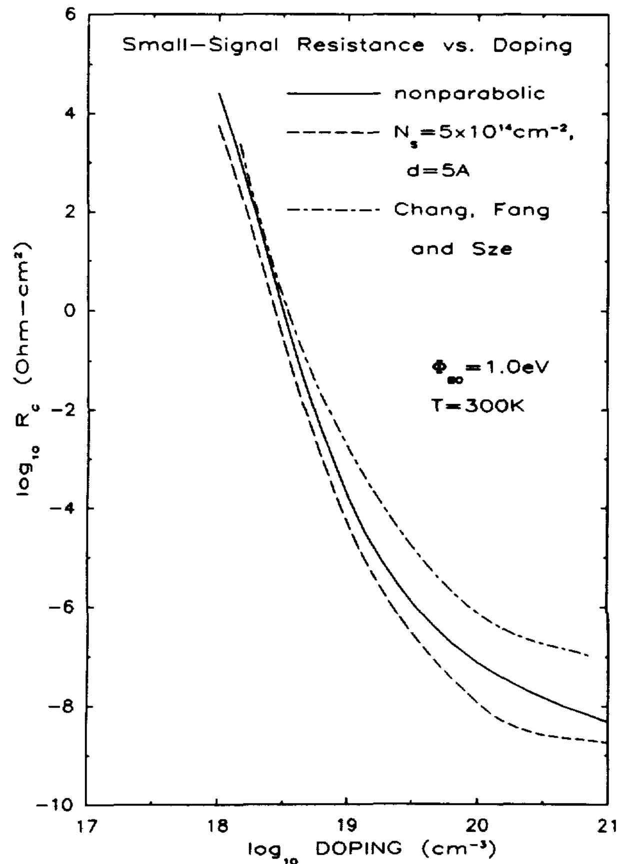

FIG. 5. Specific contact resistance vs doping, for $\phi_B = 1.0$ eV and $V = 0$ V, with and without negative surface charge, with the results from CFS.

model for $\phi_{B0} = 0.6$ and 1.0 eV. Thus we may consider the doping range from 10^{18} to 10^{19} cm^{-3} as a transition from a Schottky barrier to an Ohmic contact. As a final point of similarity, note that CFS's results and our nonparabolic curves (with no surface charge) tend to merge for dopings near 10^{18} cm^{-3}. This is to be expected, since the two models differ in their expressions for the tunneling transmission, and hence should yield the same results when the tunneling contribution is small.

Next, consider the difference between the results of the two models. The nonparabolic curves tend to lie below CFS's curves for dopings greater than 10^{18} cm^{-3}. Between dopings of 10^{18} and 10^{19} cm^{-3}, our nonparabolic curves fall with steeper slope, and continue doing so up to 10^{21} cm^{-3}, whereas by 10^{20} cm^{-3} the slopes on CFS's curves are much reduced. Thus the gap between the nonparabolic and CFS's curves increases with increasing doping. That the differences between the curves increases with doping is expected, since the tunneling contribution dominates the conductance, and the change in the function relating the imaginary part of the wavevector to the energy plays an important role, and accounts for most of the changes. Thus, at high dopings ($> 10^{19}$ cm^{-3}) it may be possible to obtain metal–semiconductor junctions with substantially lower contact resistance than previously thought feasible.

To illustrate the relative importance of the various factors in our theory, consider Fig. 4. For dopings below 10^{18} cm^{-3} or greater than 10^{20} cm^{-3}, there is negligible difference

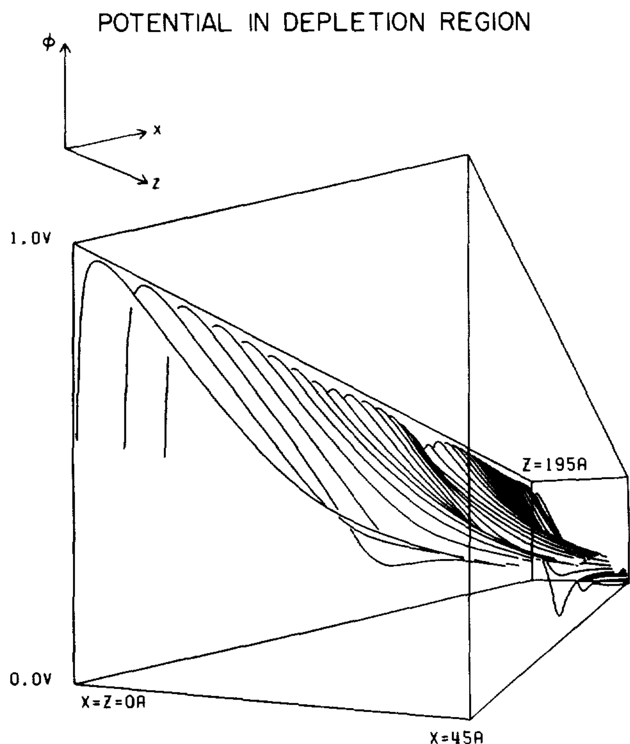

FIG. 6. Potential in the depletion region, for doping $= 8\times 10^{19}$ cm^{-3}, $\phi_B = 0.8$ eV, and $V = 0$ V. The x direction is normal to the interface and the z direction is along the interface, with resolutions of 0.5 and 1.0 Å, respectively. Also, the direction is in the ⟨100⟩ direction of the lattice.

between the parabolic and nonparabolic results. Indeed, between these doping limits, the difference is less than 0.2 on the log scale. [That the parabolic curve falls below the nonparabolic curve is obvious from Eq. (9).] By our choice of parameters for the surface charges, greater difference is seen between this curve and the nonparabolic curve than between that and the parabolic curve. Qualitatively, including surface charges causes little difference, except at dopings greater than 10^{20} cm^{-3}, where the curve flattens. The reason for this can be seen from Fig. 2. At 10^{20} cm^{-3}, the negative surface charges have greatly reduced the barrier. Effectively, there is no barrier, so further increases in doping will have little effect. Quantitatively, we may say that the presence of any negative surface charge will accentuate the difference between our results and CFS's results. The effect of neglecting image-force lowering is slight; it causes the curves to shift upwards slightly by ~0.2.

IV. FLUCTUATIONS

One significant effect that has not been included in this theory is fluctuations in the potential due to the discreteness in the doping. A simple Monte Carlo model has been used to calculate the fluctuations, wherein dopants have been randomly placed as substitutional impurities within a GaAs lattice, in the depletion region. One such result is illustrated in Fig. 6, for a doping of 8×10^{19} cm^{-3} and $\phi_{B0} = 0.8$ eV. The potential is shown in a 45 Å × 195 Å rectangle in an xz plane, where x is normal to the interface and z is parallel to the interface. The potential is seen to exhibit significant variations. In a future paper,[17] we shall describe our model, and calculate the effects of such fluctuations on the conductance as a function of doping, and compare these to the results presented here.

V. CONCLUSION

We have presented a model for the calculation of contact resistance and conductance as a function of energy of the tunneling electron, for a metal-n-GaAs junction, where the GaAs is heavily doped, so that tunneling is significant. This model uses the WKB approximation and the two-band model to obtain a nonanalytic expression for the transmission probability. The contact resitance at zero bias is compared with that from CFS's model. We suggest that our model determines the transmission probability more accurately than CFS's model, which assumes constant transmission for all tunneling energies.

ACKNOWLEDGMENTS

We would like to gratefully acknowledge the support of the Office of Naval Research under Contract No. N00014-82-K-0556. We would also like to thank A. Zur and G. Y. Wu for their advice. One of us (WJB) is the recipient of a Hackett Studentship from the University of Western Australia.

[1]P. A. Barnes and A. Y. Cho, Appl. Phys. Lett. **33**, 651 (1978).
[2]C. Y. Chang, Y. K. Fang, and S. M. Sze, Solid State Electron. **14**, 541 (1971).
[3]J. G. Werthen and D. R. Scifres, J. Appl. Phys. **52**, 1127 (1981).
[4]R. L. Mozzi, W. Fabian, and I. J. Piekarski, Appl. Phys. Lett. **35**, 337 (1979).
[5]N. Braslau, J. Vac. Sci. Technol. **19**, 803 (1981).
[6]S. M. Sze, *Physics of Semiconductor Devices* (Wiley, New York, 1981), Chap. 5.
[7]G. H. Parker, T. C. McGill, C. A. Mead, and D. Hoffman, Solid State Electron. **11**, 201 (1968).
[8]J. W. Conley and G. D. Mahan, Phys. Rev. **161**, 681 (1967).
[9]D. R. Fredkin and G. H. Wannier, Phys. Rev. **128**, 2054 (1962).
[10]J. W. Conley, C. B. Duke, G. D. Mahan, and J. J. Tiemann, Phys. Rev. **150**, 466 (1966).
[11]D. J. BenDaniel and C. B. Duke, Phys. Rev. **152**, 683 (1966) (see also Ref. 9).
[12]E. O. Kane, *Physics of III–V Compounds* (Academic, New York, 1966), Vol. 1, Chap. 3.
[13]K. S. Kunz, *Numerical Analysis* (McGraw-Hill, New York, 1957).
[14]C. D. Thurmond, J. Electrochem. Soc. **122**, 1133 (1975).
[15]J. S. Blakemore, J. Appl. Phys. **53**, R123 (1982).
[16]R. H. Fowler and L. W. Nordheim, Proc. R. Soc. London Ser. A **119**, 173 (1928).
[17]W. J. Boudville and T. C. McGill (unpublished).